

Anisotropy in the Arrival Directions of Ultrahigh-Energy Cosmic Rays

Luis Villaseñor

Benemérita Universidad Autónoma de Puebla, Puebla, Mexico, on leave of absence from UMSNH, Morelia, Mexico

E-mail: lvillasen@gmail.com

Abstract. In this article we illustrate, in an interactive way, the analysis and visualization of anisotropy properties in the arrival directions of ultrahigh-energy cosmic rays detected by the Telescope Array and the Pierre Auger experiments by using data released by both collaborations. We describe the use of several programs that we have written in Python and Julia languages for this purpose. We also discuss the potential sources and analyse the effect of correcting the arrival directions to take into account the deflections of the cosmic rays by the magnetic field of our galaxy for one specific model of the galactic magnetic field under several assumptions about the composition of the primary cosmic rays.

1. Introduction

One of the most important results in the field of ultrahigh-energy cosmic rays (UHECRs) is the discovery of a hotspot in the arrival directions of the highest-energy cosmic rays detected with the Telescope Array (TA) experiment in the northern sky [1]. In this article we describe a number of programs that we have written in Python and Julia that can be used to reproduce these results by using the data that the Telescope Array Collaboration has made public. In their paper they use Li-Ma [2] significances, in this article we show that the use of P_{value} produces the same results.

Since these lectures were given at the VI School on Cosmic Rays and Astrophysics [3] our emphasis was on providing the students with a complete set computational tools required to reproduce these results and to eventually use these tools to make new progress on their own, this article illustrates the use of all the programs in detail. This software was available to everybody during the lectures.

The measurement of the statistical significance of the deviation from isotropy in the arrival directions of the highest-energy cosmic rays, and in particular, the calculation of penalty factors to account for the search for such deviations, can benefit from the use of high performance computing (HPC) on a cluster of CPUs and, for that reason, we provided an elementary introduction to Monte Carlo (MC) methods and the use of the Message Passing Interface (MPI) library [4]. In the lectures we made extensive use of the Jupyter Notebook as an interactive environment to work with software code, plots, data, websites, etc., and for that reason we also provided an elementary introduction to the use of the Jupyter Notebook [5], previously known as IPython Notebook.

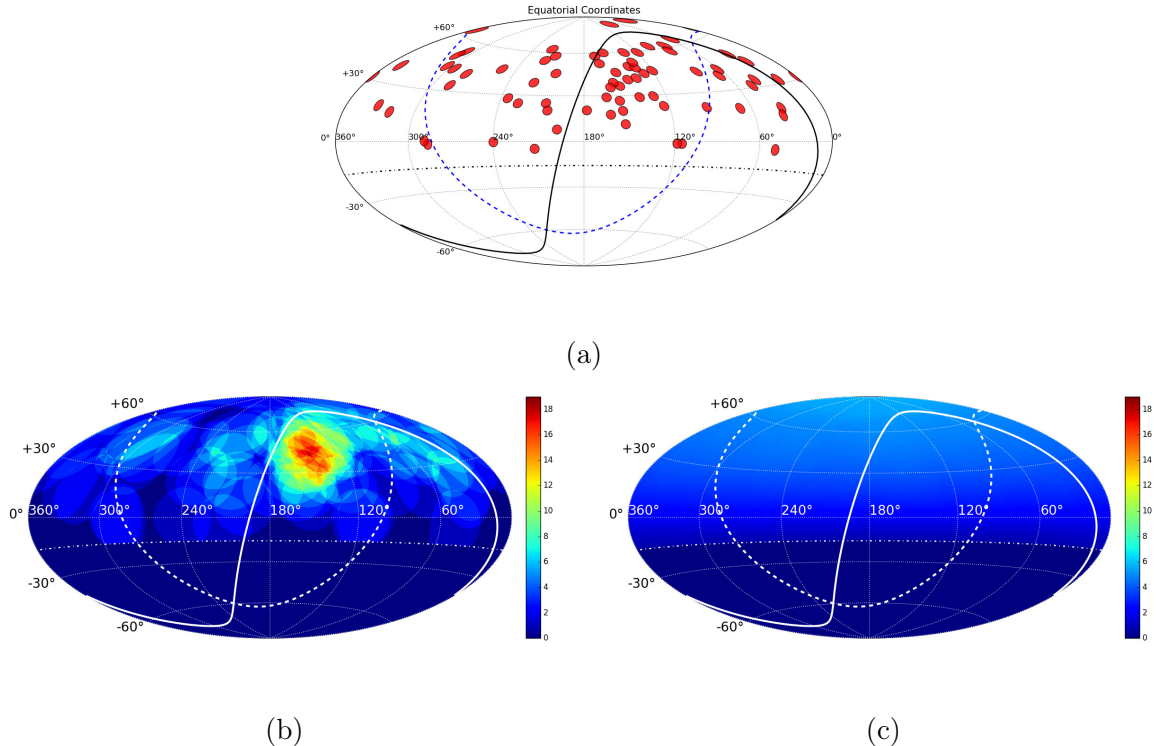


Figure 1: Maps in equatorial coordinates using the Hammer projection for the data detected by the Telescope Array experiment [1]. The solid curve represents the supergalactic plane and the dashed line represents the galactic plane. The dotted line indicates the limit of the field of view of the TA experiment. (a) 72 UHECR events detected with $E \geq 57$ EeV and zenith angle $< 55^\circ$. (b) Same events oversampled with $R = 20^\circ$. (c) One hundred thousand isotropic MC events generated in the field of view of the TA experiment, oversampled with $R = 20^\circ$ and normalised to 72 events.

The same procedure and programs were used during the lectures to reproduce the anisotropy results in the arrival directions of the highest-energy cosmic rays in the southern sky [6] reported by the Pierre Auger Collaboration .

In addition, we describe the source code that we have written to backpropagate these cosmic rays, from the Earth to the edge of our galaxy, in the presence of galactic magnetic fields. We use the Julia language and apply it to a particular model of the galactic field for different assumptions about the composition of the primary cosmic rays.

The programs described in this article are presently available for download [7] and can be used freely by anyone, they have been tested in Mac OS X and Ubuntu operating systems. Finally, in order to facilitate the use of this article in an interactive way, the commands used to produce the results, and to create the plots, are shown in blue.

2. Hotspot Discovered by the Telescope Array Experiment

The hotspot in the arrival directions of ultrahigh-energy cosmic rays, discovered by the Telescope Array Collaboration in the northern sky, was reported in [1] for energies above 57 EeV with a statistical significance of 3.4σ . In this section we use the data released by the TA Collaboration in [1] to reproduce their results with our own analysis software.

2.1. Data Sample

The data for the arrival directions of the UHECRs detected by the TA experiment can be downloaded in a complete form from the electronic edition their paper. These data consist of 72 events with $E > 57$ EeV and zenith angle $\theta < 55^\circ$ recorded from 2008 to 2013. The following data are provided for each event: date and time of occurrence, measured zenith angle, measured energy, and the equatorial coordinates of the arrival direction given by right ascension (RA or α) and declination (DEC or δ).

2.2. Data analysis

We will follow the analysis procedure described in [1]. First we copy the data and save it in a file named `TA_AstrophysJLett_2014.dat`. The format of this file can be displayed by the following command:

```
head -5 TA_AstrophysJLett_2014.dat
```

which produces the following output:

```
#Date and Time (UTC) Zenith(deg) E(EeV) RA(deg) DEC(deg)
2008 Jun 10 17:05:37 46.91 88.8 93.50 20.82
2008 Jun 25 19:45:52 31.98 82.6 68.86 19.20
2008 Jun 29 08:22:45 41.20 101.4 285.74 -1.69
2008 Jul 15 05:26:31 34.26 57.3 308.45 53.91
```

Next we change a few dashes for minus signs, convert from equatorial to galactic coordinates, apply some cuts and visualise the events with the program `PlotEvents.py`:

```
python PlotEvents.py TA
```

which creates the plot shown in Fig. 1.a.

In order to follow the same anisotropy analysis described in [1] we must now perform an oversampling with a radius of 20° around every point in the sky by using a grid of $0.1^\circ \times 0.1^\circ$. This time we use the Julia language to speed up the calculations and we optimise our code through the use of the k-dimensional tree algorithm[8]. The Julia program that we use for this purpose is named `OverSample.jl`; the command to oversample the TA events with a radius= 20° is the following:

```
julia OverSample.jl TA 20
```

this program creates an oversampled map of the Telescope Array events and stores it in the file named `N_on.dat`. Next we use the program `PlotMap.py` to visualise this map with the command:

```
python PlotMap.py TA
```

which creates the plot shown in Fig. 1.b.

The next step consists in the evaluation of the background noise under the assumption that this noise is isotropic. For this purpose we generate 100 000 simulated arrival directions, taking into account the geometrical exposure as a function of zenith angle, θ , for the Telescope Array given by Eq. 1.

$$\frac{d\Omega}{dN} = N_o \sin\theta \cos\theta \quad (1)$$

The program that generates these Monte Carlo events is called `MCSim.jl`, we therefore execute the command:

```
julia MCSim.jl
```

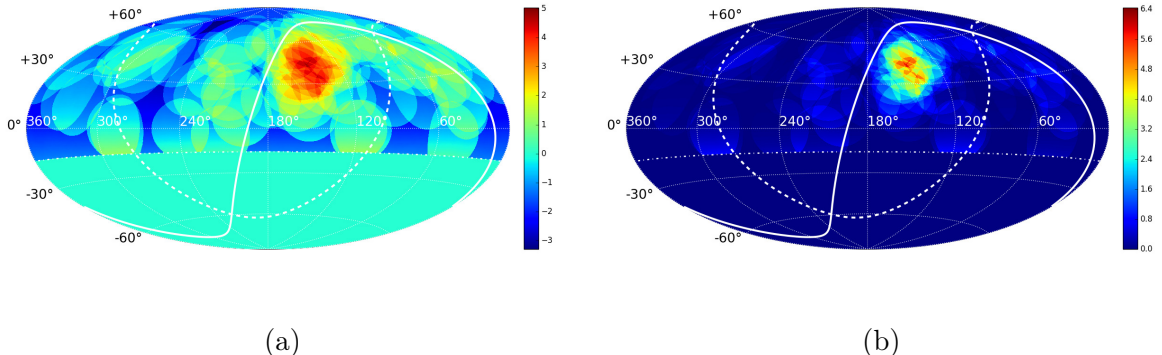


Figure 2: Maps in equatorial coordinates using the Hammer projection for the data detected by the Telescope Array experiment [1]. The solid curve represents the supergalactic plane and the dashed line represents the galactic plane. The dotted line indicates the limit of the field of view of the TA experiment. (a) Map of the Li-Ma significance defined in Eq. 2. (b) Map of P_{value} defined in Eq. 3 and Eq. 4.

which creates a text file named `100K_evts.txt`. Next we apply the same oversampling procedure that we applied to the data and normalise to a total of 72 events. We therefore run again the program `OverSample.jl`, but this time applied to MC data simulated in the field of view of the TA experiment:

```
julia OverSample.jl Sim_TA 20
```

this program creates an oversampled map of the MC isotropic events generated in the field of view of the Telescope Array experiment with the same grid of 1800×3600 points and the same oversampling radius of 20° that we used for the data. The map generated is stored in the file named `N_off.dat`.

Since the number of events is higher, the execution of this program takes a few minutes in a typical laptop. One alternative to speed it up is to use MPI to parallelise the execution in case one can use a multiprocessor computing system.

In turn we use the program `PlotMap.py` to visualise this map with the command:

```
python PlotMap.py Sim_TA
```

that creates the plot shown in Fig. 1.c, the scale of its color bar is adjusted to match that of Fig. 1.b.

2.3. Statistical significance based on S_{LM}

Now we proceed to use both the oversampled data, `N_on.dat` shown in Fig. 1.b, and the oversampled isotropic background, `N_off.dat` shown in Fig. 1.c, to quantify the deviation from isotropy present in the data.

For this purpose we use the value of the Li-Ma significance [2], denoted by S_{LM} , calculated for each pixel by means of Eq. 2, where $\alpha = 72/100000$ is the ratio of the number of events in the data sample to the number of isotropic MC events.

$$S_{LM} = \left[2N_{on} \ln \left(\frac{(1 + 1/\alpha)N_{on}}{N_{on} + N_{off}} \right) + 2N_{off} \ln \left(\frac{(1 + \alpha)N_{off}}{N_{on} + N_{off}} \right) \right]^{1/2} \quad (2)$$

We use the program named `LiMaSigma.jl` through the following command:

```
julia LiMaSigma.jl TA
```

this program produces the following output:

```
Max Val S_LM=5.04
Max Val -log10(P_VALUE)=6.45
```

and creates the files named `S_LM.dat` that in turn can be visualised with the `PlotMap.py` program as follows:

```
python PlotMap.py S_LM_TA
```

to generate the Li-Ma significance map shown in Fig. 2.a.

2.4. Statistical significance based on P_{value}

An alternative to the use of the Li-Ma significance is the use of P_{value} [9] to measure the deviation from isotropy. The P_{value} is defined in Eq. 3 and Eq. 4.

$$P_{value} = P_{Poisson}(X \geq N_{on}) \quad (3)$$

$$P_{value} = 1 - CDF_{Poisson}(\mu = \alpha N_{off}, X = N_{on} - 1) \quad (4)$$

where $CDF_{Poisson}$ is the Poisson cumulative distribution function.

The program `LiMaSigma.jl` that we run above also generated the P_{value} significance map `P_value.dat` which can be visualised with the following command:

```
python PlotMap.py P_value_TA
```

shown in Fig. 2.b.

In order to measure the statistical significance of the hotspot we now simulate a large number of sets of MC 72 events generated isotropically and we find out that only a fraction of 3.7×10^{-4} have a $\sigma_{LiMa} > 5.1$. We also find that the same fraction of sets have a $P_{value} < 10^{-6.4}$ meaning that using P_{value} is equivalent to using S_{LM} . These numbers correspond to a statistical significance of 3.4σ one-sided.

3. Hotspot Discovered by the Pierre Auger Observatory in the Southern Sky

The code we have used to reproduce the hotspot discovered with the Telescope Array experiment can be applied straightforwardly to the data released by the Pierre Auger Collaboration in 2015 [6] which also exhibits a hotspot located at $RA = 198.0^\circ$ and $DEC = -25.2^\circ$ in the southern sky, although with a lower statistical significance.

First we copy the data released in [6] and save it in a file named `Auger_AstrophysJ804_2015.dat`. The format of this file can be displaying by printing a few lines with the following command:

```
head -5 Auger_AstrophysJ804_2015.dat
```

which produces the following output:

```
#Year JulianDay Zenith(deg) E(EeV) RA(deg) DEC(deg) l(deg) b(deg)
2004 125 47.7 62.2 267.2 -11.4 15.5 8.4
2004 142 59.2 84.7 199.7 -34.9 -50.8 27.7
2004 177 71.5 54.6 12.7 -56.6 -56.9 -60.5
2004 239 58.3 54.0 32.7 -85.0 -59.1 -31.8
```

Next we change dashes for minus signs, apply some cuts and visualise the events with the program `PlotEvents.py`:

```
python PlotEvents.py Auger
```

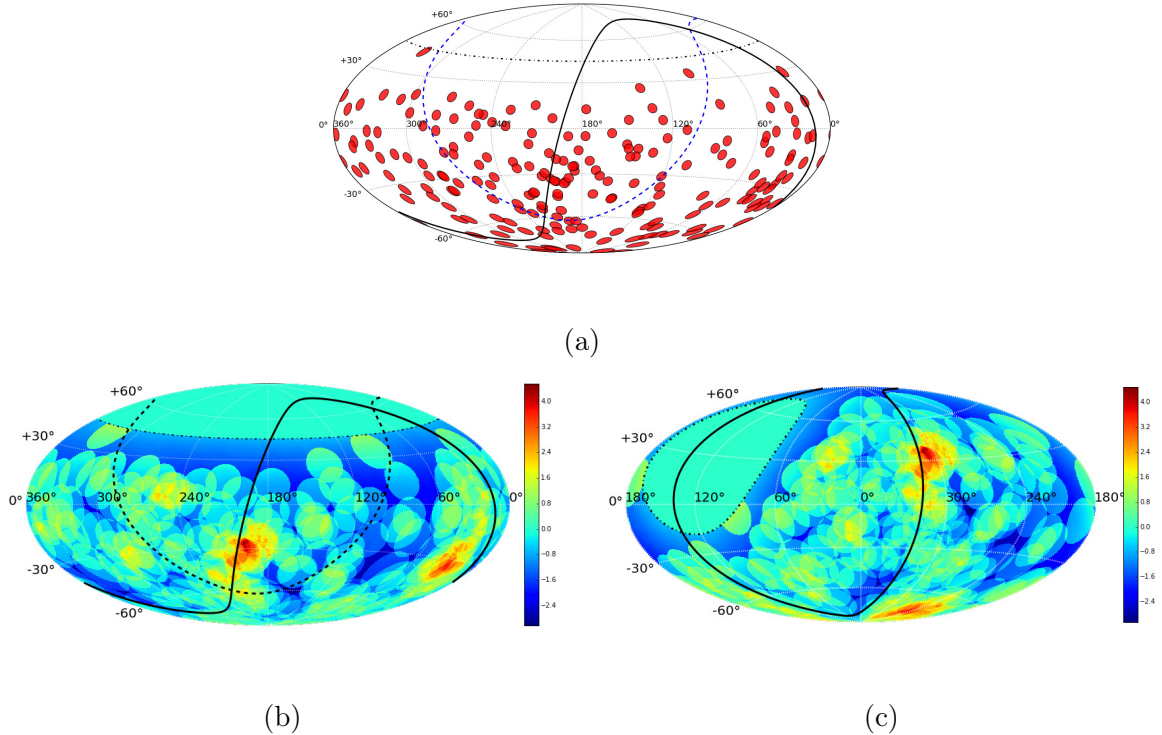


Figure 3: Maps using the Hammer projection for the data realeased by the Pierre Auger Collaboration [6]. The solid curve represents the supergalactic plane and the dashed line represents the galactic plane. The dotted line indicates the limit of the field of view of the Pierre Auger Observatory. (a) Map in equatorial coordinates of the 200 UHECR events detected with $E \geq 54$ EeV and zenith angle $< 80^\circ$. (b) Map in equatorial coordinates of the Li-Ma significance defined in Eq. 2 for an oversampling radius of 12° . (c) Same as Fig. 3.b but in galactic coordinates.

which creates the plot shown in Fig. 3.a.

The same procedure and same programs as those described above can be used to measure σ_{LM} and P_{value} . Fig. 3.b shows the Li-Ma significance map in equatorial coordinates for an oversampling radius of 12° and Fig. 3.c shows the same Li-Ma significance map in galactic coordinates. The maximum value $\sigma_{LM} = 4.6$ occurs at $RA = 198.0^\circ$ and $DEC = -25.2^\circ$. Application of a penalty factor to account for the search procedure reduces the statistical significance as discussed in [6].

4. Potential Sources of Ultrahigh-Energy Cosmic Rays

In search of a correlation with the positions of potential astrophysical sources of the UHECRs we use the Swift BAT 70-Month Hard X-ray Survey, available from [10], which includes 1210 hard X-ray sources with the majority of them classified as AGN.

First we can copy these data with the command:

```
 wget http://swift.gsfc.nasa.gov/results/bs70mon/inc/data/BAT_70m_catalog_20nov2012.txt
```

To read these data we use:

```
 python Read_BAT_Swift.py
```

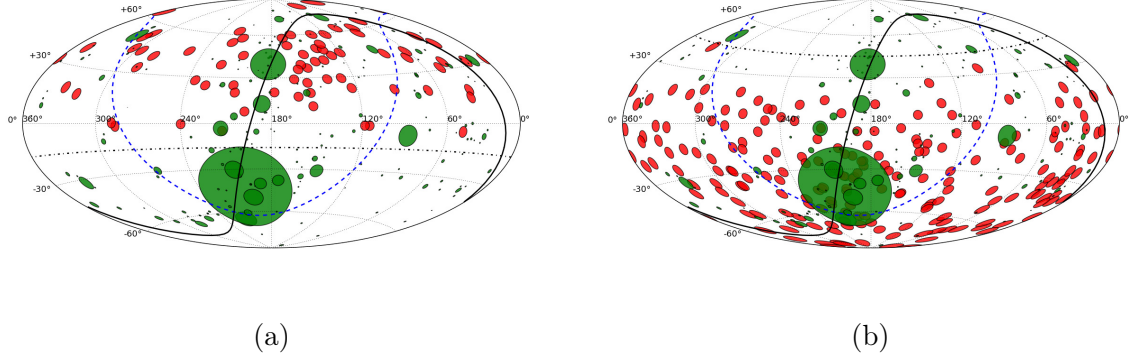


Figure 4: Maps in equatorial coordinates using the Hammer projection of displaying the arrival directions of UHECR events and the positions of objects from the Swift BAT 70-Month Hard X-ray Survey. The solid curve represents the supergalactic plane and the dashed line represents the galactic plane. The red circles have a radius of 3° and represent the detected events. The green circles represent the 202 objects located within 100 Mpc from the Earth, their radii are arbitrarily scaled as $Flux/50$ in degrees. (a) Events detected by the Telescope Array experiment previously shown in Fig. 1.a . (b) Events detected by the Pierre Auger Observatory previously shown in Fig. 3.a.

which produces the following output with the flux listed in descending order for the 202 objects with $redshift < 0.0235$ (roughly equivalent to a $distance < 100$ Mpc) :

Total number of objects=	1210			
Total number of objects with measured redshift < 0.0235=	202			
Name RA DEC Flux Redshift				
Cen A	201.38	-43.03	1388.99	0.0018
NGC 4151	182.67	39.42	538.93	0.0033
NGC 2110	88.04	-7.43	319.13	0.0078
IC 4329A	207.32	-30.33	290.49	0.016
NGC 4945	196.34	-49.47	284.86	0.0019
NGC 4388	186.45	12.68	277.38	0.0084
Circinus Galaxy	213.29	-65.33	272.12	0.0014
NGC 5506	213.31	-3.24	241.03	0.0062
MCG -05-23-016	146.93	-30.94	201.3	0.0085
4C 50.55	321.18	50.95	200.46	0.02
NGC 4507	188.87	-39.89	188.11	0.0118
NGC 3783	174.76	-37.74	181.11	0.0097
NGC 7172	330.5	-31.87	170.93	0.0087
Mrk 348	12.22	31.96	156.04	0.015
Mrk 3	93.84	71.04	140.96	0.0135
MCG +08-11-011	88.76	46.45	133.44	0.0205
NGC 3516	166.66	72.58	118.34	0.0088
AX J1737.4-2907	264.37	-29.15	115.86	0.0214
NGC 5252	204.58	4.54	115.48	0.023
ESO 103-035	279.56	-65.44	111.73	0.0133
.....				
2MASX J18305065+0928414	277.71	9.48	3.11	0.019

where RA and DEC are measured in degree, and the flux, measured by BAT-Swift in the 14-195 KeV band, is measured in units of $10^{-12} \text{ ergs cm}^{-2}\text{s}^{-1}$.

Next we proceed to make a map of these potential sources of UHECRs superimposed on the Telescope Array events by typing the following command:

```
python PlotEvents.py TA Cat
```

which produces the plot shown in Fig. 4.a.

Likewise, we can make a map of these potential sources superimposed on the Auger events with the command:

```
python PlotEvents.py Auger Cat
```

which creates the plot shown in Fig. 4.b.

The radii displayed for the Swift BAT 70-Month Hard X-ray Survey are arbitrarily scaled. In the absence of a model, we use weights that are directly proportional to the absolute luminosity measured in the 14-195 KeV band, in such a way that the D^2 factor in the absolute luminosity cancels out with the D^2 in the denominator due to the solid angle that our Galaxy presents as a target. Therefore we use $R = \text{Flux}/50$ in degrees with Flux in $10^{-12} \text{ ergs cm}^{-2}\text{s}^{-1}$ for the radii of these astrophysical objects, and $R = 3^\circ$ for the radii of the events.

We arbitrarily limit the redshift of the plotted objects to < 0.0235 which corresponds to 100 Mpc when we convert with [11]. Note that using redshifts as a measure of distance is only a first approximation as it excludes possible motions of the objects within their local gravitational fields, a better approximation would be to use the measured distances available in [12].

Fig. 4 suggests that, assuming that the production of UHECRs is correlated with the production of hard X rays in the energy band measured by BAT-Swift (14-195 KeV), the hotspot observed in the northern sky can be explaining as dominated by two sources, namely NGC 4151 and NGC 4388, displayed in the northern sky of Fig. 4.a as green circles with radii 10.8° and 5.6° , respectively, whereas the southern hotspot, reported by Auger with a lower statistical significance, can be attributed to a few sources, namely CenA, NGC 2110, IC 4329A, NGC 4945, the Circinus Galaxy and NGC 5506, displayed in the southern sky of Fig. 4.b as green circles with radii equal to 27.8° , 6.4° , 5.8° , 5.7° , 5.4° and 4.8° , respectively. The fact that the northern sky has fewer potential sources in this context may explain its more compact hotspot with respect to the southern sky.

A similar exercise could be done using the Veron Catalog of Quasars & AGN, 13th Edition [13]. However this catalog is known to be statistically incomplete and non-uniform, although for sources within 100 Mpc the incompleteness and the non-uniformity may not represent a problem, another inconvenience of the Veron Catalog is the poor precision on the redshifts assigned to the AGN, although this can be easily fixed by using the more precisely measured distances available from [12].

5. Correction due to the Galactic and Extragalactic Magnetic Fields

The dream of doing astronomy with UHECRs, based on the assumption that the deflections of the cosmic rays at these extreme energies would be small enough to point to the sources, has gradually disappeared as we collect more data. This means that either the cosmic rays are light nuclei but the galactic and extragalactic fields are more intense than expected, or the composition is dominated by heavy nuclei, or both.

As we gradually discover more details about the intensities and structures of the galactic and extragalactic magnetic fields, and improve on the measurement of the composition of the primary cosmic rays, we will, in principle, apply better corrections that may eventually lead to the identification of the most important sources. In addition, the knowledge about the potential sources derived from multi-messenger approaches will lead to a better understanding of the acceleration mechanisms, as well as the ranges of energies and the nature of the primaries.

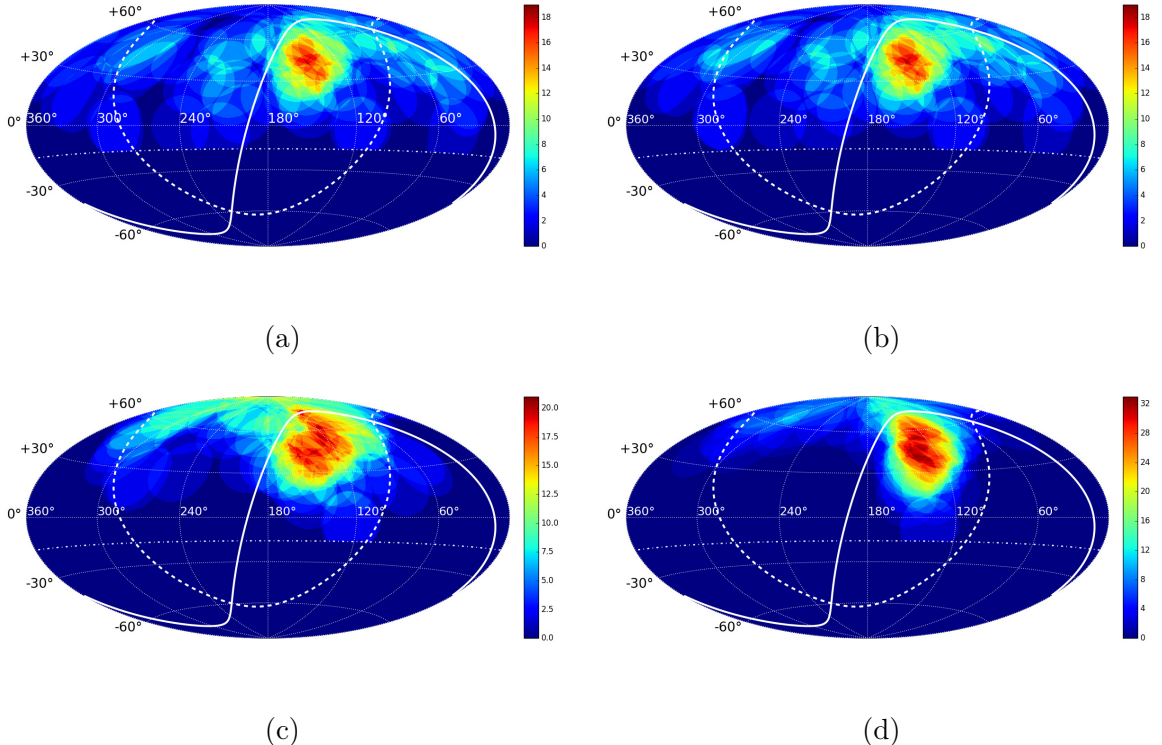


Figure 5: Maps in equatorial coordinates using the Hammer projection for the UHECR events detected by the Telescope Array experiment [1]. The solid curve represents the supergalactic plane and the dashed line represents the galactic plane. The dotted line indicates the limit of the field of view of the TA experiment. The oversampling radius is 20° in all plots. In (b), (c) and (d) the galactic magnetic field is approximated by the regular component of the JF2012 model. (a) Original events. (b) Events backpropagated to the edge of the Galaxy assuming pure proton composition. (c) Events backpropagated to the edge of the Galaxy assuming pure oxygen nuclei composition. (d) Events backpropagated to the edge of the Galaxy assuming pure iron nuclei composition.

In this section we describe the use of the required computational tools to correct for the deflections of the detected UHECRs in the presence of a particular model of the galactic magnetic field, called JF2012 and derived from fits to the WMAP7 Galactic Synchrotron Emission map and more than forty thousand extragalactic rotation measures [14, 15].

In particular we describe the use of a set of programs, written in Julia language and including Bash scripts, to backpropagate charged particles from the Earth to the edge of the Milky Way galaxy. We use the JF2012 model for the galactic magnetic field and use different assumptions about the composition of the UHECRs detected by the TA and the Pierre Auger collaborations.

The program named `CRBackProp.jl` uses the adaptive Cash-Karp method [16] to solve the Lorentz force equation to obtain the trajectories of the backpropagated UHECRs and the program `Propa_JF2012.jl` translates the JF2012 model into Julia code. Other alternative programs to backpropagate cosmic rays are [17] and [18].

As an example, if we want to backpropagate an iron nuclei that arrives with an energy of 60 EeV from the direction *galactic longitude* = 40° and *galactic latitude* = -20° , we run the Julia program named `CRBack_Prop_example.jl` listed here:

```
include("JF2012.jl")
```

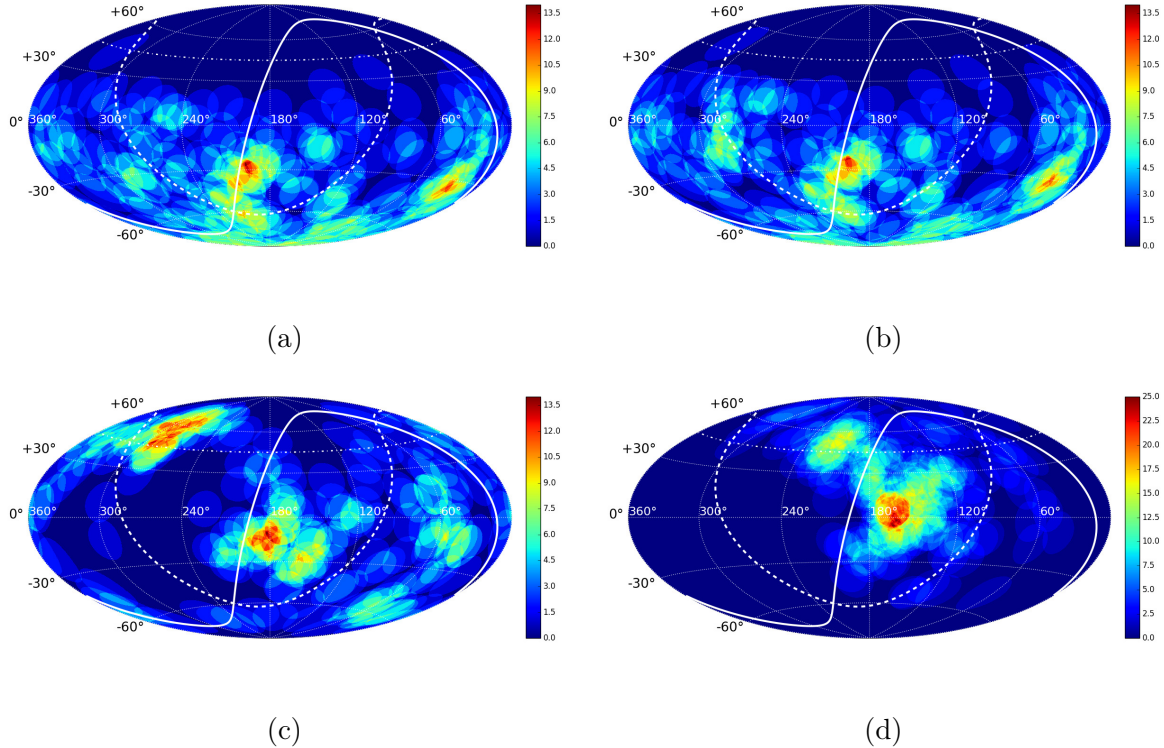


Figure 6: Maps in equatorial coordinates using the Hammer projection for the UHECR events detected by the Pierre Auger Observatory [6]. The solid curve represents the supergalactic plane and the dashed line represents the galactic plane. The dotted line indicates the limit of the field of view of the Auger experiment. The oversampling radius is 12° in all plots. In (b), (c) and (d) the galactic magnetic field is approximated by the regular component of the JF2012 model. (a) Original events. (b) Events backpropagated to the edge of the Galaxy assuming pure proton composition. (c) Events backpropagated to the edge of the Galaxy assuming pure oxygen nuclei composition. (d) Events backpropagated to the edge of the Galaxy assuming pure iron nuclei composition.

```
include("Cash-Karp.jl")
include("Propa_JF2012.jl")
alpha = Propa_JF2012(26,56,60.,40.,-20.,1,true,false,false,20000.)
```

This program produces the following output:

```
niter  niter_advance  E_f  x_f  y_f  z_f  l_f  b_f  alpha  t_f
101    94  60.01 1326.01 19344.98 6714.38 86.07 19.09 59.72 66980.37
```

returning the number of iterations, the energy (in EeV), the positions of the particle (in pc), the galactic longitude and galactic latitude of the entrance direction at the edge of the Galaxy (in degrees), the deflection between the entrance direction at the edge of the Galaxy and the arrival direction at the Earth (in degrees) and the time to transit our galaxy (in years).

In order to backpropagate all the events detected by the TA experiment we use the Bash script named `Backprop.sh`. Assuming all the detected events are protons we backpropagate them by using the following sequence of commands:

```
python PlotEvents.py TA
sh Backprop.sh p
```

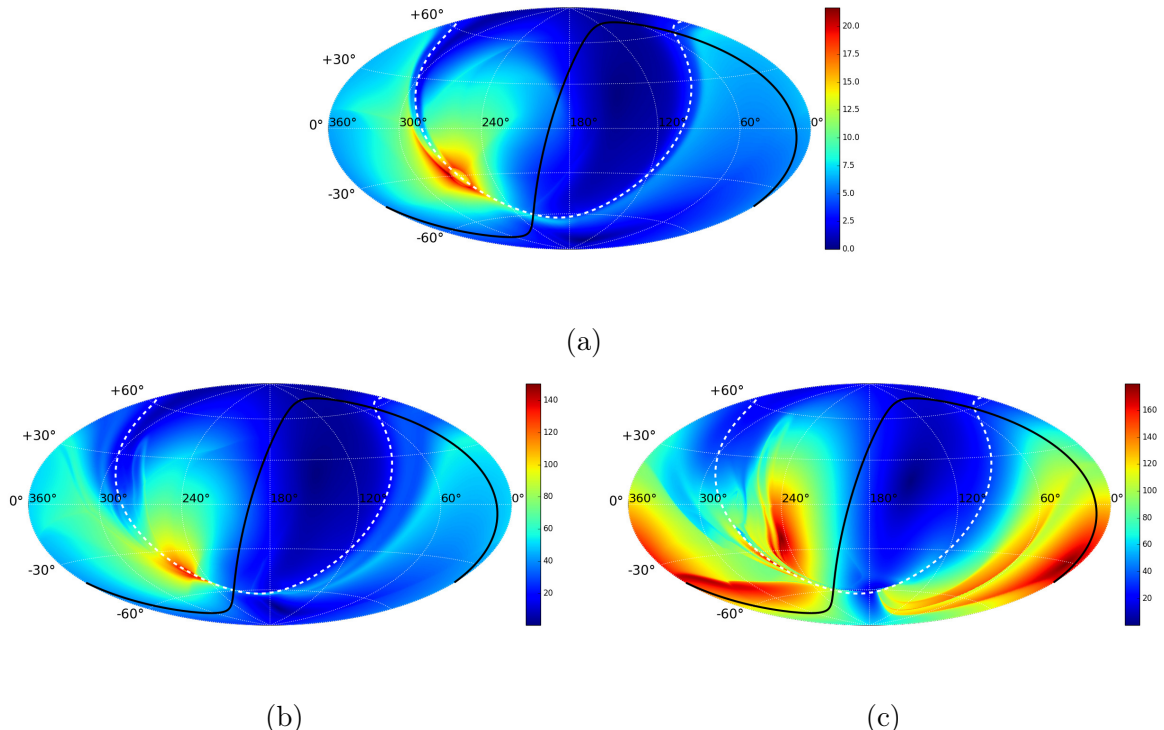


Figure 7: Deflection angles in degrees for particles arriving at each point of these maps with $E = 60$ EeV. These particles are backpropagated to the edge of the Galaxy with the galactic magnetic field approximated by the regular component of the JF2012 model. All the maps are in equatorial coordinates using the Hammer projection. The solid curve represents the supergalactic plane and the dashed line represents the galactic plane. (a) Assuming the particles are protons. (b) Assuming the particles are oxygen nuclei. (c) Assuming the particles are iron nuclei.

which produces a file named `Data.p.jf2012.dat`. Next we use the following sequence of commands:

```
python PlotEvents.py TA p
julia Oversample.jl TA 20
```

to oversample with a radius = 20° , and finally the command:

```
python PlotMap.py TA
```

to create a plot with the oversampled map for the backpropagated events. If we backpropagated these events under the assumption that they are oxygen or iron nuclei we simply replace `p` by `O` or `Fe`, respectively, in the above sequence of commands.

The procedure described gives rise to the plots shown in Fig. 5 under the assumptions that all the UHECRs are protons, oxygen nuclei or iron nuclei, respectively. Note that we have used only the so-called regular component of the field in the JF2012 model, but one can activate the striated and/or the turbulent component of the model as well. This is done by changing one or the two `false` variables to `true` in the call to the function `Propa_JF2012`.

In a similar way we obtain the oversampled maps for the backpropagated events detected by the Pierre Auger Observatory, according to [6] this time we use an oversampling radius = 12° ; to do this we just replace `TA` by `Auger` in the sequence of commands given above. The results are shown in Fig. 6.

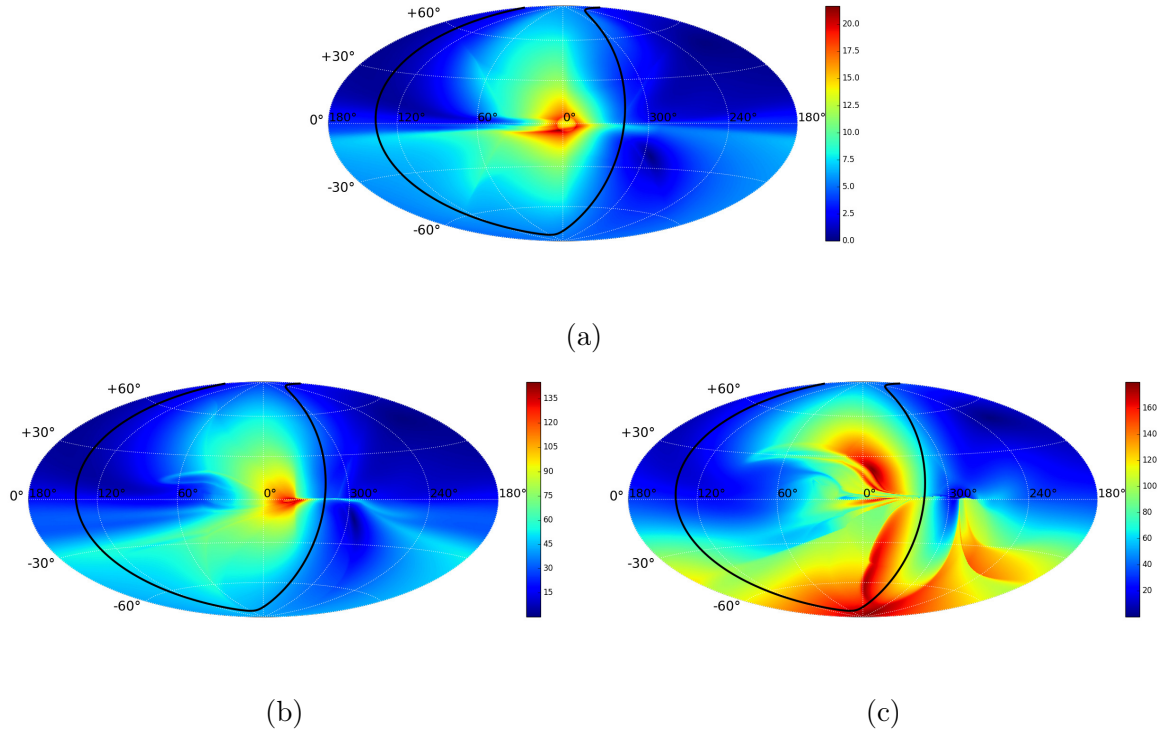


Figure 8: Deflection angles in degrees for particles arriving at each point of these maps with $E = 60$ EeV. These particles are backpropagated to the edge of the Galaxy with the galactic magnetic field approximated by the regular component of the JF2012 model. All the maps are in galactic coordinates using the Hammer projection. The solid curve represents the supergalactic plane. (a) Assuming the particles are protons. (b) Assuming the particles are oxygen nuclei, (c) Assuming the particles are iron nuclei.

We can conclude that both hotspots, in the northern and southern sky, are magnified if we take into account the deflections produced by the galactic magnetic field, approximated by the JF2012 model, under the assumption of a composition dominated by medium or heavy nuclei. The positions of the hotspots are near the positions of the uncorrected hotspots, and both are on the same side of the supergalactic plane. We are in the process of adding the deflections due to the extragalactic magnetic model using some of the proposed models for the latter.

Above we suggested the idea that the lower compactness of the southern hotspot may be due to the contribution of more sources from the Swift BAT 70-Month Hard X-ray Survey with respect to the northern sky, this idea may be reinforced if the different potential sources accelerate predominantly different particles at these extreme energies leading to more disperse angular deflections due to the galactic and extragalactic magnetic fields.

It is evident that a more quantitative correlation study is required to reinforce or discard some of these ideas. Likewise, it will be very interesting so study the effect in the positions and compactness of the hotspots due to the inclusion of deflections caused by extragalactic magnetic fields.

6. Maps of Deflection Angles due to the Galactic Magnetic Field for the JF2012 Model

By using the same Julia programs described above we can backpropagate cosmic rays of a fixed energy for different compositions. To do this, we divide the full sky in a grid of $180 \times 5 \times 360 \times 5$ points, i.e., we use the *granularity* variable equal to 5 instead of 10 as we previously did, and backpropagate protons, oxygen nuclei and iron nuclei arriving at the points of this grid with an energy of 60 EeV. The back propagation to the edge of the Galaxy assumes a galactic magnetic field approximated by the regular component of the JF2012 model.

Given that we need to backpropagate over 1.6 million particles, and since their trajectories are independent, we use MPI [4] in a multiprocessor HPC cluster to speed up the execution of this task which is trivially parallelizable. We use the following commands:

```
mpirun -n N -machinefile hosts julia mpi_map.jl EQ
```

and

```
mpirun -n N -machinefile hosts julia mpi_map.jl Gal
```

to obtain deflection maps in equatorial and galactic coordinates, respectively. The file `hosts` contains the names of the nodes of your cluster to use a total of N cores, where N can be small or large depending on your computing resources.

Fig. 7 shows the maps of deflections for protons, oxygen nuclei and iron nuclei of 60 EeV backpropagated in equatorial coordinates and Fig. 8 shows the same in galactic coordinates.

7. Conclusions

In this article we have described the use of a number of programs that we have written in Python and Julia that can be used to reproduce data analyses that lead to the discovery of a hotspot in the arrival directions of the highest-energy cosmic rays detected with the Telescope Array experiment in the northern sky, and also to reproduce the findings of the Pierre Auger Collaboration in the southern sky. We do this by using data released by both collaborations.

We have also described the use of programs that can be used to correlate the arrival directions of the detected events with the locations in the sky of possible sources from the Swift BAT 70-Month Hard X-ray Survey.

We have also presented the analysis of the effect of correcting the arrival directions, reported by both experiments, to take into account the deflections of the cosmic rays caused by the magnetic field of our galaxy. We have described the use of these programs for one specific model of the galactic magnetic field under several assumptions about the composition of the primary cosmic rays.

In particular we have shown that both hotspots, in the northern and southern skies, are magnified if we take into account the deflections produced by the galactic magnetic field, approximated by the JF2012 model, under the assumption of a composition dominated by medium to heavy nuclei. The positions of the corrected hotspots are near the positions of the uncorrected hotspots and both are on the same side of the supergalactic plane. It will be interesting to add deflections due to extragalactic magnetic fields using some of the proposed models for the latter that may eventually move the hotspots closer to the supergalactic plane, and closer to the potential sources mentioned above, namely CenA, NGC 2110, IC 4329A, NGC 4945, the Circinus Galaxy and NGC 5506 in the southern sky and NGC 4151 and NGC 4388 in the northern sky.

Finally, we have presented maps, in equatorial and galactic coordinates, of deflections of protons, oxygen nuclei and iron nuclei, of a fixed energy equal to 60 EeV, when they are backpropagated to the edge of our galaxy in a galactic magnetic field approximated by the regular component of the JF2012 model.

The programs that we have written for the analyses described in this article can be used freely by anybody, they can be downloaded from [7].

Appendix A: Installation of Python Modules

The use of Python may become unstable due to the accidental use of conflicting libraries, for this reason it is recommended to install a virtual environment though the use of *virtualenv* [19] which is a tool to create isolated Python environments. A simpler solution is to install the Python distribution from *anaconda* [20] and then type

```
conda update conda  
conda create -p CR python matplotlib basemap ipython
```

next you can activate the CR Python environment with the command:

```
source activate /YOUR-PATH/CR
```

The next step is to install the specific python modules required by using the *pip* command associated to the active virtual environment by means of the following commands:

```
pip install astrophysics  
pip install CosmoloPy  
pip install pandas
```

next you can download astroconvert from [21] or use the following command:

```
wget http://vanderbiltastro.pbworks.com/w/file/fetch/46335397/astroconvert.py
```

If you want to go back to use your normal Python environment you just deactivate the CR environment with the command:

```
source deactivate /YOUR-PATH/CR
```

Appendix B: Installation of the Julia Language and Required Packages

The Julia language is a relatively new high-level, high-performance dynamic programming language created specifically for technical computing. It can be installed by downloading the appropriate file and following the platform specific instructions from [22]. We recommend to use version 0.4.2 to assure compatibility with the KDTree package. If you want to use the MPI package it is necessary to install first the OpenMP application programming interface [23], check the installation instructions specific to your platform. The required packages to run the described programs in Julia can be installed by typing the commands:

```
julia  
Pkg.add("KDTree")  
Pkg.add("SkyCoord")  
Pkg.add("MPI")
```

Acknowledgements

The author thanks CONACyT for making possible the creation of the Center for High Performance Computing of UMSNH in Morelia, and the Laboratorio Nacional de Supercómputo del Sureste de México, located in the BUAP Campus in Puebla; the Monte Carlo simulations of this article were performed in these facilities. The author also thanks CONACyT for the support during his leave of absence from UMSNH and for support received through the Mesoamerican Centre for Theoretically Physics located in Tuxtla Gutierrez, Chiapas, Mexico.

References

- [1] R. U. Abbasi et al. [Telescope Array Collaboration], *Astrophys. J. Lett.* 790, L21 (2014)
- [2] T. Li and Y. Ma, *ApJ*, 272 (1983) 317
- [3] http://mctp.mx/e_VI_School_on_Cosmic_Rays_and_Astrophysics.html
- [4] <http://dl.acm.org/citation.cfm?id=898758>
- [5] <https://ipython.org/notebook.html>
- [6] A. Aab et al. [Pierre Auger Collaboration], *Astrophys.J.* 804 (2015) 1, 15
- [7] <https://github.com/lvillasen/ToolsCosmicRays>
- [8] Bentley, J. L., "Multidimensional binary search trees used for associative searching". *Communications of the ACM*. 18 (1975) 9.
- [9] Bhattacharya, Bhaskar; Habtzghi, DeSale (2002). "Median of the p value under the alternative hypothesis". *The American Statistician*.
- [10] <http://swift.gsfc.nasa.gov/results/bs70mon/>
- [11] <http://roban.github.io/CosmoloPy/>
- [12] NASA/IPAC Extragalactic database, <http://ned.ned.caltech.edu/forms/byname.html>
- [13] <http://heasarc.gsfc.nasa.gov/W3Browse/galaxy-catalog/veroncat.html>
- [14] R. Jansson and G. R. Farrar, A New Model of the Galactic Magnetic Field, *ApJ* 757 (2012) 14.
- [15] R. Jansson and G. R. Farrar, The Galactic Magnetic Field, *Astrophys. J.* 761 (2012) L11.
- [16] J. R. Cash, A. H. Karp. "A variable order Runge-Kutta method for initial value problems with rapidly varying right-hand sides", *Transactions on Mathematical Software* 16: 201-222, 1990.
- [17] M.S. Sutherland, B.M. Baughman, J.J. Beatty, *Astroparticle Physics*, Volume 34, Issue 4, p. 198-204. (2010)
- [18] R.A. Batista, M. Erdmann, C. Evoli, K.-H. Kampert, D. Kuempel, G. Müller, G. Sigl, A. van Vliet, D. Walz, T. Winchen, *EPJ Web of Conferences* 99 (2015) 13004
- [19] <https://virtualenv.pypa.io/en/stable/>
- [20] <https://www.continuum.io/downloads>
- [21] <http://vanderbiltastro.pbworks.com/w/file/46335397/astroconvert.py>
- [22] <http://julialang.org/downloads/>
- [23] <http://openmp.org/wp/>